Asian Journal of Chemistry; Vol. 26, No. 17 (2014), 5527-5530

ASIAN JOURNAL OF CHEMISTRY

http://dx.doi.org/10.14233/ajchem.2014.18148

Molding Method of Polymethylmethacrylate Microstructures *via* Laser Melting†

W.S. TAN*, J.Z. ZHOU, S. HUANG and W.L. ZHU

Center for Photon Manufacturing Science and Technology, School of Mechanical Engineering, Jiangsu University, Zhenjiang 212013, P.R. China

*Corresponding author: Tel: +86 13776892977; E-mail: tws.163@163.com

AJC-15737

In order to meet the processing requirements for multiscaled, intricately shaped and high-precision polymer microstructures, this paper presented a molding method based on laser melting and also designed and developed the experimental devices. With CO_2 laser radiation, experiments of microstructure molding on PMMA substrates were conducted. By establishing theoretical models and software simulations, this research analyzed specimen temperature changes in the laser scanning process and carried out an orthogonal experiment to analyze the effects of processing parameters on parts quality. Results show that effects of processing parameters on parts quality are as follows: Laser power plays a decisive role in the repetition accuracy. The influencing results of scanning times were also significant, followed by mold temperature and compaction pressure. Optimized technological parameters, such as a laser beam diameter of 20 mm, scanning velocity of 15 mm/s, laser power of 2.7 W, scanning time of 18 s, compaction pressure of 100 N and a mold temperature of 70 ºC, were adopted to obtain molds with high repetition accuracy and a microstructure dimensional deviation of less than 1 µm.

Keywords: CO_2 laser, Melting molding, Microstructured parts, Replication precision.

INTRODUCTION

Polymer parts with microstructures are a key part of micro electromechanical systems (MEMS) and microanalysis systems which show extensive material parameters and unique microstructure characteristics different from other materials[1,2]. In the early 1990s, micro processing methods were first applied in MEMS. Since then, polymer micro processing has been acknowledged as an increasingly important technique. Becker *et al.*[3,4] and Giboz *et al.*[5] summarized the polymer micro processing approach and pointed out that polymer microfabrication generally includes hot embossing, microinjection molding, micromolding and laser ablation. The micromolding process is complex and can only be applied to thermosetting plastics[6]. Microinjection molding and hot embossing are the main replication methods for most kinds of thermoplastics. However, hot embossing has a long cycle time and injection molding requires expensive and complex devices.

In recent years, ultrashort laser etching of polymer substrates was introduced, such as the femtosecond laser and excimer laser for etching PMMA[7]. However, its etching rate is low and the costs are high, especially for large-scale etchings. On the contrary, PMMA microstructure processing by CO_2 laser ablation is highly efficient. Mohammed *et al.*[8] and Qi *et al.*[9] conducted a research using the industrial CO_2 Laser device in the ablation of PMMA microfluidic chips. The parameters include a laser power of 10-60 W, scanning velocity of 80-400 mm/s and a typical microchannel width of 50-250 ìm. However, defects induced by photothermal effects can appear in the CO_2 laser ablation regions, such as protrusion, spatter and re-solidification[10,11]. These defects create certain impacts on the surface roughness and cross-section shapes of the microchannels.

At present, CO_2 laser thermal effects can be applied for microchannel ablation, surface modification and cutting and welding of polymer substrates[12-14]. Yet there are limited studies on polymer microstructure molding done by laser melting. In this paper, a fast polymer melting molding device was developed. At room temperature, the CO_2 laser scanned and melted the PMMA substrate. The laser scanning and molding time were controlled in 30 s and the entire processing cycle was less than 60 s.

EXPERIMENTAL

The microstructure was designed as nine continuous ripples each measuring 620 µm wide and 160 µm tall. The

†Presented at 2014 Global Conference on Polymer and Composite Materials (PCM2014) held on 27-29 May 2014, Ningbo, P.R. China

size of the PMMA specimen was 14 mm(L) × 10 mm(W) × 1 mm (H) processed by laser cutting. The PMMA parameters included the CO_2 laser absorption coefficient of 92 %, thermal conductivity of 0.19 W/(m k), specific heat of 1420 J/kg K, density of 1190 kg/m^3, glass transition temperature (T_g) of 105 ºC, flow temperature of 140 ºC, thermal degradation temperature of 270 ºC and ablation temperature of 340 ºC.

The laser device was an industrial machine capable of a continuous output CO_2 laser (CLS2000, Chendu, Instrument Inc., China), with a laser wavelength of 10.64 μm and laser power of 0-50 W. A laser beam with a diameter of 0.15-20 mm was obtained by adjusting the lens. The mould was mainly made of the restraint layer, template, mold core, temperature controller, elevator and pressure controller. The restraint layer was made of ZnSe window glass that showed a CO_2 laser transmittance rate of 99 %. The mold core was made of die steel and electric sparks were used in the precise processing of the microstructure features.

This study also used a digital microscope system (VHX-1000, Japan) to test the microstructure features of the mold core and molded parts. Fig. 1(a) shows an image of the mold core. The microstructural three-dimensional shape of the mold core is shown in Fig. 1(b). The width (C-D) of the ripple was measured. The cross-section of the middle ripple was 621.3 μm and its height was (A-B) 163.3 μm.

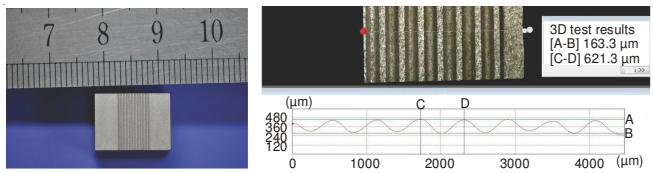

Fig. 1. Topography of the mold core. (a) Photograph of mold core (b) Microstructural cross-section of mold core

Experimental process: The basic experimental process is shown in Fig. 2. The PMMA specimen was placed in the mould cavity and the laser scanning pathway and scanning velocity were set. Laser beams were irradiated on the specimen surface through the restraint layer and the specimen temperature rapidly increased and produced the melt. The melt was compacted in the mould to form the microstructure. The specific operation is as follows:

The adjusted laser parameters were: a power of 2.0-2.7 W, laser beam diameter of 20 mm, scanning velocity of 15 mm/s and an overlapped light spot center and center of specimen surface. The light spot was scanned in a roundtrip manner along the central line in the length direction on the specimen surface. The scanning and melting process showed with the power set at 2.5 W, the light spot was scanned for 10 s in a roundtrip method when the specimen reached a softened state. After 10-15 s of roundtrip scanning, the specimen was completely melted. Any scanning times longer than 20 s resulted in specimen thermal degradation, which was consistent with previous experimental results of laser melting polymer.

With the laser beam and scanning velocity remaining unchanged from the descriptions mentioned above, different powers and scanning times were attempted for the laser melting. When the specimen was melted, the compaction pressure was

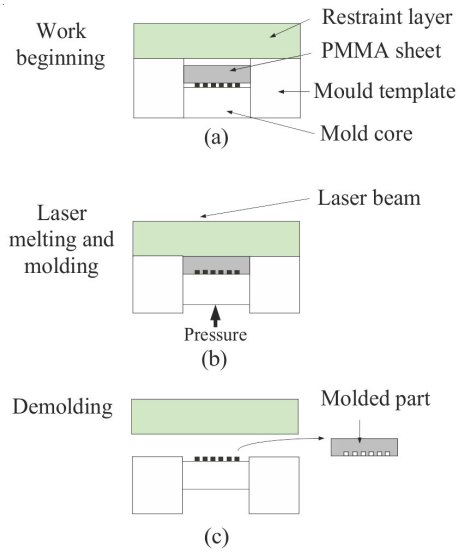

Fig. 2. Schematic diagram of the laser-melted mold. (a) Setup (b) Laser melting and molding (c) De-molding

loaded at 50-150 N and held for 30 s. When the specimen temperature decreased and the specimen returned to a solid state, the part was removed from the mould. The entire processing cycle was less than 60 s.

With parameters set at a mold temperature of 70 ºC, a compaction pressure of 150 N and laser power of 2.5 W, the microstructural three-dimensional shape and cross-sectional dimensions of the obtained molding pieces at scanning times of 10 and 15 s are illustrated in Fig. 3(a,b), respectively. At the same test location (in the fifth ripple in the middle), the following sizes were generated: Fig. 3(a): 579.5 μm wide and 74.2 μm tall, Fig. 3(b): 616.9 μm wide and 149.8 μm tall. Morphology and dimensions of the mold core microstructures in Fig. 3 were compared, showing increased laser scanning time and reduced microstructure size deviation in the moldings.

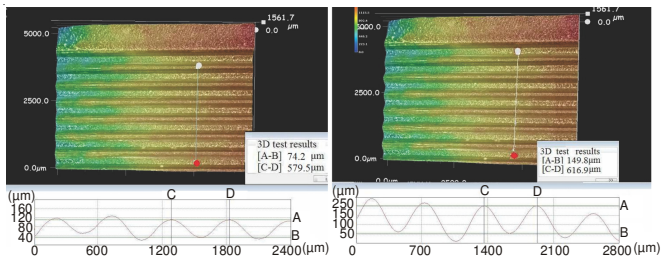

Fig. 3. Cross-section profiles of the molded parts. (a) 2.5 W for 10 s (b) 2.5 W for 15 s

RESULTS AND DISCUSSION

Effects of specimen temperatures

Numerical model of laser melting specimen: In laser-melted moldings, the specimen temperature is the key to the microstructure molding. This experiment used the basic mode of the CO_2 laser and the beam energy showed Gaussian distribution. The power density of the light beams can be calculated using the following equation:

$$P_{(x,y)} = \frac{2P_0}{\pi r^2}\exp\left(-2\frac{x^2+y^2}{r^2}\right) \quad (1)$$

where P_0 is the laser power and r is the radius of the laser beam. The material performance was assumed to be isotropic and the beams were vertically directed on to the specimen surface. The specimen surface absorbed the laser energy and the heat transfer abided by Fourier's law. The beam was radiated forward along the x-axis at velocity v. The specimen temperature field and the heat conduction equation of the light spot adjacent area at t are as follows:

$$T_{(x,y,z,t,v)} - T_0 = \frac{2\rho P_0 \sqrt{a}}{k\pi^{3/2}} \times \int_0^t \frac{dt'}{\sqrt{t-t'}[8a(t-t')+r^2]}$$

$$\exp\left[-2\frac{(x-vt')^2+y^2}{8a(t-t')+r^2} - \frac{z^2}{4a(t-t')}\right] \quad (2)$$

$$\frac{\partial}{\partial x}\left(k\frac{\partial T}{\partial x}\right) + \frac{\partial}{\partial y}\left(k\frac{\partial T}{\partial y}\right) + \frac{\partial}{\partial z}\left(k\frac{\partial T}{\partial z}\right) + P_{(x,y)} = \frac{\partial}{\partial t}(c\rho T) \quad (3)$$

where c is the thermal capacity, ρ is the material density, k is the thermal conductivity and a is the laser absorption coefficient. Eqns. 1-3, as well as the initial conditions (t = 0, T = T_0, T_0 as ambient temperature) were considered to solve the temperature field distribution at t.

Software simulation: The specimen temperatures during the laser scanning process were analyzed using finite element software Comsol. Firstly, the finite element model was established. The lengths and widths of the specimens were slightly smaller than the mould cavity. It can also be considered that only the specimen bottom contacted the mould. The boundary and loading conditions were set at an initial temperature of 20 ºC, laser power of 2.5 W, beam diameter of 20 mm and scanning velocity of 15 mm/s. The model and simulation results are shown in Fig. 4. Fig. 4(a) is the 3D result of specimen temperature after 5 s of laser scanning. The specimen temperature was distributed in the range of 50-140 ºC. The temperature in each region of the specimen did not reach the melting temperature. After 10 s of laser scanning, the temperature distribution on the cross-section of the specimen is shown in Fig. 4(b). The specimen temperature fell in the range of 80-190 ºC. On the section, there was over one-third of the area with a temperature above 140 ºC and the specimen was locally melted. After 20 s of laser scanning, the range of the specimen temperature was approximately 150-260 ºC, as shown in Fig. 4(c), which indicates that the sample was melted completely.

According to the simulated specimen temperatures and molded parts obtained from experiments, it was found that the microstructure size deviation was mainly produced by the Gaussian laser beams and the graded distribution of the specimen temperature. In addition, because the melt temperature influences the part quality, the higher the specimen temperature is, the better the degree of duplication.

Effects of processing parameters

Orthogonal experiment design: Using the numerical simulations and experiment results, Minitab software was used to design the orthogonal experiment. Under the conditions of the laser beam and scanning velocity, the possible influencing factors adopted in this experiment included the laser power,

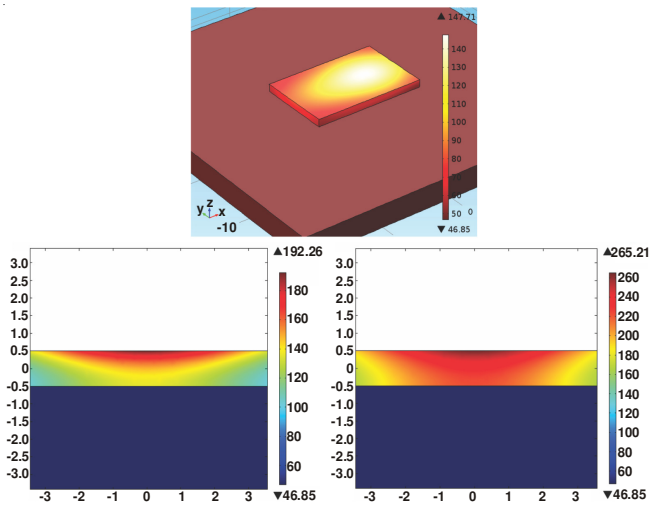

Fig. 4. Simulation of temperature distribution with different scanning times. (a) 5 s (b) 10 s (c) 20 s

scanning time, mold temperature and compaction pressure. For each factor, three levels were applied. The relationship between each factor and each level are shown in Table-1. To facilitate the analysis of the effects of processing parameters on part quality, the differences of the microstructure waveform heights between the parts and mold core was defined as repetition accuracy.

TABLE-1
EXPERIMENTAL FACTORS AND LEVELS

Level	Laser power (W)	Scanning time (s)	Molding pressure (N)	Mould temperature (ºC)
1	2.0	10	50	50
2	2.5	15	100	60
3	2.7	20	150	70

As the microstructured parts were longer along the longitudinal ripple direction, the middle ripple was selected for the evaluation of height deviation. In this study, the arrangement of the orthogonal experiment, data recording and computational results are listed in Table-2. As shown in the principle coefficient response in Table-3, the laser power was the decisive factor that influenced the repetition accuracy of the microstructure. Scanning times and mold temperatures were secondary factors. The compaction pressure was relatively less influential than the other factors.

TABLE-2
ORTHOGONAL EXPERIMENT DESIGN AND TEST RESULTS

Number	Laser power (W)	Scanning time (s)	Molding pressure (N)	Mould temperature (ºC)	Molding deviation (μm)
1	2.0	10	50	50	96.6
2	2.0	15	100	60	82.5
3	2.0	20	150	70	53.7
4	2.5	10	100	70	21.2
5	2.5	15	150	50	10.3
6	2.5	20	50	60	15.6
7	2.7	10	150	60	2.5
8	2.7	15	50	70	6.7
9	2.7	20	100	50	0.3

TABLE-3
RESPONSE TABLE OF DATA MEANS

Level	Laser power (W)	Scanning time (s)	Molding pressure (N)	Mould temp. (ºC)
1	1.981	1.998	1.712	1.811
2	1.732	1.751	1.635	1.792
3	1.643	1.711	1.773	1.754
Delta	0.460	0.259	0.067	0.196
Rank	1	2	4	3

The levels of the selected factors were correlated with indicators as required and the deviation was as small as possible. The levels that could reduce the indicator were applied, which was the minimum size deviation. Therefore, level three laser power, level three scanning time, level two compaction pressure and level three mold temperature were combined. The optimal technological parameter combination was adjusted as follows: laser beam diameter of 20 mm, scanning velocity of 15 mm/s, laser power of 2.7 W, scanning time of 18 s, compaction pressure of 100 N and mold temperature of 70 ºC. The microstructure of the PMMA substrate obtained from the experiment is presented in Fig. 5. Fig. 5 shows better microstructure shape consistency between the molded part and the mould. The dimension deviations were 3.8 μm in width and 0.5 μm in height.

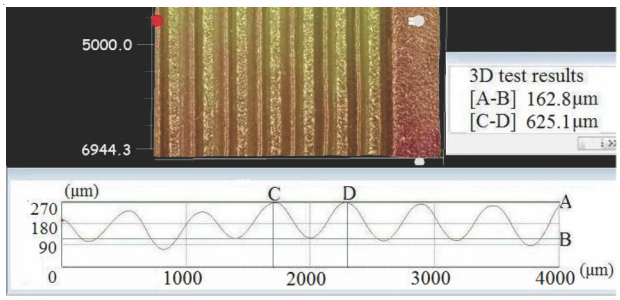

Fig. 5. Cross-section of the microstructures using the optimal parameters

Conclusion

This paper proposed a new molding method of polymer microstructures using a laser technique. With this approach, the polymer was irradiated by a low-power CO_2 laser and absorbed the laser energy. Polymer temperature quickly exceeded the glass transition temperature (T_g), but stayed below the thermolysis temperature. The melt was directly shaped inside the mould by compaction. Numerical simulation and experimental results demonstrated that the melting temperature is a key factor that influences molding quality, as high temperature leads to a good molding precision. A satisfactory repetition accuracy of the microstructure was obtained by optimizing the processing parameters, which indicates that polymer microstructure molding by laser melting is possible.

ACKNOWLEDGEMENTS

This work was financially supported by National Nature Science Foundation of China (No. 51175236), Jiangsu Province 2013 "333 Project" funded project and the Innovative Plan Project of College Graduate Student of Jiangsu Province China (CXZZ11_0545).

REFERENCES

1. M.I. Mohammed and M.P.Y. Desmulliez, *Lab Chip*, **11**, 569 (2011).
2. Y.-W. Chen, H. Wang, M. Hupert, M. Witek, U. Dharmasiri, M.R. Pingle, F. Barany and S.A. Soper, *Lab Chip*, **12**, 3348 (2012).
3. H. Becker and C. Gärtner, *Anal. Bioanal. Chem.*, **390**, 89 (2008).
4. H. Becker and U. Heim, *Sens. Actuators A Phys.*, **83**, 130 (2000).
5. J. Giboz, T. Copponnex and P. Mélé, *J. Micromech. Microeng.*, **17**, 96 (2007).
6. N. Qi, Y. Luo, X. Yan, X. Wang and L. Wang, *Microsyst. Technol.*, **19**, 609 (2013).
7. A. Costela, I. Garciamoreno, F. Florido, J.M. Figuera, R. Sastre, S.M. Hooker, J.S. Cashmore and C.E. Webb, *J. Appl. Phys.*, **77**, 2343 (1995).
8. M.I. Mohammed, E. Abraham and M.P. Desmulliez, *J. Micromech. Microeng.*, **23,** 035034 (2013).
9. H. Qi, X.S. Wang, T. Chen, X.M. Ma and T.C. Zuo, *Microsyst. Technol.*, **15**, 1027 (2009).
10. J.M. Li, C. Liu and L.Y. Zhu, *J. Mater. Process. Technol.*, **209**, 4814 (2009).
11. D.G. Waugh and J. Lawrence, *Opt. Lasers Eng.*, **48**, 707 (2010).
12. Y.G. Huang, S.B. Liu, W. Yang and C.X. Yu, *Appl. Surf. Sci.*, **256**, 1675 (2010).
13. J.B. Lei, Z. Wang and Y.S. Wang, *Chin. J. Lasers*, **40**, 0103006 (2013).
14. J.P. Davim, C. Oliveira, N. Barricas and M. Conceição, *Int. J. Adv. Manuf. Technol.*, **35**, 875 (2008).